

Impact of Thermal Boundary Resistance on Laser Inclusion Damage

J. P. Longtin,* T. Q. Qiu,† and C. L. Tien‡
University of California at Berkeley, Berkeley, California 94720

The present work rigorously analyzes the effect of thermal boundary resistance (TBR) on laser heating of an inclusion embedded in a nonabsorbing optical medium. The TBR impedes the flow of heat across the inclusion/medium interface, enhances the inclusion heating rate, and reduces the laser damage threshold. The results indicate that in some cases the damage threshold is only half of that predicted when the boundary resistance is neglected. Both an exact solution and approximate scaling relations are developed that incorporate the TBR. The scaling relations show that when the TBR is considered, the damage threshold can have a stronger dependence on the pulse width than previously predicted.

Introduction

THE past decade has seen significant advances in short-pulse, high-power laser technology. Current laser intensities have reached 10^{19} W/m² and are projected to increase by several orders of magnitude in the near future.¹ Many novel applications exist for these lasers including laser material processing, high temporal and spatial resolution measurements, and laser fusion. One of the biggest obstacles in the application of these lasers is radiation damage incurred by optical components (windows, prisms, etc.) in the laser system. One laser damage mechanism is the so called *inclusion-induced* damage model. Essentially, inclusions—physical impurities in an otherwise pure optical component material—absorb high-intensity electromagnetic radiation and convert this radiation to thermal energy, causing the inclusion to heat up. As the inclusion temperature increases, the surrounding (host) material attempts to conduct the thermal energy away. If the host material cannot adequately conduct away this thermal energy, and the host or inclusion temperature exceeds some threshold temperature—e.g., the melting temperature of the host material, the vaporization temperature of the particle, or a particle temperature that causes fracture in the host—then permanent damage to the optical component can result.^{2–4} Inclusion-dominated damage is particularly prevalent in thin film applications where the inclusion density is much higher than that of the bulk film material.³ In the following, *particle* refers to the absorbing inclusion embedded within the nonabsorbing (i.e., dielectric) host optical material, which is called the *medium*.

To quantify the damage process, damage thresholds are assigned to optical components that characterize the laser radiation limits the component can safely tolerate without sustaining damage. This work is unique in that the thermal boundary resistance (TBR) between the particle and host medium is incorporated in a laser damage model that predicts the damage threshold of optical media. The TBR increases the heating rate of the inclusion and reduces the damage threshold of the optical material. Also, the TBR effect in-

creases as the heat flux across the interface increases, which becomes particularly important as technology advances in the past decade have resulted in lasers with increasingly shorter pulse widths that produce tremendously high heat fluxes in the materials they interact with.

Thermal Boundary Resistance

Heat flow across an interface between dissimilar materials results in a temperature drop at the interface. This temperature drop is found to be proportional to the heat flux across the interface; thus, an interfacial thermal resistance—called the TBR—can be defined as⁵

$$R_{bd} = (\Delta T / \dot{Q}) \quad (1)$$

where R_{bd} is the TBR, ΔT the temperature drop across the interface, \dot{Q} the total heat flow across the interface, and A the area normal to the heat flow.

One source of TBR is imperfect mechanical contact at the interface that results from irregularities on the mating surfaces of each material. This results in a net reduction of the effective interfacial area available for heat transfer, which constricts heat flow and results in an interfacial resistance, often called the *contact resistance*.^{6,7} This resistance depends on several factors including the pressure between the two materials. Higher pressure results in more severe deformation of the contact surfaces, increasing the contact area and reducing the TBR.

Another source of TBR is phonon reflection at the interface. Only a fraction of the phonons, which are quantized lattice vibrations,⁸ incident on one side of the interface is transmitted to the other side.⁹ The remaining phonons are reflected back into the original medium. The fraction of phonons reflected (or transmitted) depends on the density and sound velocity differences between the two materials. Phonon reflection is a quantum mechanical effect and is usually associated with cryogenic temperatures; however, as the heat flux across the interface increases, this effect becomes important at higher temperatures as well. Several models of phonon reflection have been developed,^{9,10} some of which treat the interface as perfectly specular (acoustic mismatch theory) or perfectly diffuse (diffuse mismatch theory). Another novel approach by Majumdar¹¹ treats the interface as a fractal surface and addresses phonon reflection and associated TBR from such a surface. The models work well at very low temperatures, but become progressively worse as the temperature increases.

Swartz and Pohl¹² measured the TBR of a layer of Rh_{99.5}:Fe_{0.05} deposited on an Al₂O₃ substrate. They found that for temperatures above 30 K the measured R_{bd} exceeded their model

Received Sept. 9, 1993; revision received Dec. 22, 1993; accepted for publication Dec. 23, 1993; presented as Paper 94-0125 at the AIAA 32nd Aerospace Sciences Meeting and Exhibit, Reno, NV, Jan. 10–13, 1994. Copyright © 1994 by the American Institute of Aeronautics and Astronautics, Inc. All rights reserved.

*Graduate Student Researcher, Department of Mechanical Engineering, Student Member AIAA.

†Postdoctoral Fellow, Department of Mechanical Engineering.

‡A. Martin Berlin Professor of Mechanical Engineering. Fellow AIAA.

predictions, and they speculated that the additional resistance resulted from phonon scattering in a thin disordered layer in the substrate next to the interface. They quantified this idea by depositing a series of different-thickness films of SiO_2 between the Rh:Fe material and the Al_2O_3 substrate, and found that the TBR increased as the SiO_2 layer increased in thickness.

This work incorporates TBR into an inclusion-based laser damage model. No distinction is made regarding the different sources of TBR discussed above. Hopper and Uhlmann,¹² however, have speculated that TBR arising from imperfect mechanical contact is minimal because the particle expands upon heating, increasing the interfacial pressure, and reducing R_{hd} . Furthermore, because the discussed theories are not yet well developed for general applications,⁹ experimentally obtained values are used for R_{hd} .

Analysis

This section presents the development of a laser heating model that incorporates the TBR at the particle-medium interface. Appropriate assumptions and solution techniques are also discussed. For illustration purposes, Pt is used as the particle material because it has been found in optical components of high-power lasers as a result of the manufacturing process.¹³ The optical properties of Pt, expressed as $n + i\kappa$, where n and κ are the real and imaginary parts of the complex refractive index, respectively, vary considerably over the wavelengths of interest, as shown in Table 1.¹⁴ The properties of standard optical glass are used for the surrounding medium. The glass is taken to have $n = 1.5$ and $\kappa = 0$ over this wavelength range.

The density of inclusions in high-quality optical components is usually very low—Campbell et al.¹³ report values of 0.07–100 inclusions/liter; hence, the separation distance between neighboring particles is typically much greater than both the particle diameter and the radiation wavelength. As a result, the particle-radiation interaction is not strongly influenced by nearby particles, and particles are (in general) far from a boundary, allowing the approximation of a single particle embedded in a medium of infinite extent.

The temporal shape of the laser pulse is taken to be uniform, with pulse duration τ_p . Also, the time between pulse repetitions is typically several orders of magnitude longer than τ_p ; therefore, only a single pulse is considered in the heating model with the assumption that the particle-host system relaxes to equilibrium before the next heating pulse arrives.

Radiation heat transfer is not considered here because particle temperatures on the order of 10^5 – 10^6 K are required before the radiation heat flux becomes comparable to the conduction heat flux. The incident radiation is assumed to be monochromatic and unpolarized. The thermophysical properties of both the particle and medium are assumed to be temperature independent, and the particle itself is considered to be homogeneous and spherical.

Particle-Radiation Interaction

One very important consideration is how the incident laser radiation is absorbed by the particle. Fuka et al.¹⁵ incorporated two types of absorption by the particle in a laser inclusion damage model: 1) bulk (or uniform) absorption and 2) surface absorption. Bulk absorption assumes the entire particle absorbs the incident radiation uniformly, whereas surface absorption assumes most of the incident radiation is absorbed

in a thin layer near the surface of the particle. They suggested the dominant mechanism depends on the imaginary part of the complex index of refraction: surface absorption is associated with larger κ , whereas uniform absorption is assumed with smaller κ . They found that the type of absorption can affect the damage threshold somewhat.

The assumption of uniform absorption inside the particle simplifies the analysis considerably; however, this assumption can be very erroneous. For the laser damage problems of practical interest, the inclusion particle size a is often comparable to the incident radiation wavelength λ . As a result, approximate limiting conditions (i.e., for $a \ll \lambda$ or $a \gg \lambda$) cannot be generally applied, and Maxwell's equations must be used to determine the particle-radiation interaction. The most general approach considers the fields both inside and outside the particle.¹⁶ Tuntomo and Tien¹⁷ studied the radiation deposition and subsequent heating of spherical particles subjected to intense laser radiation. Their results vividly show that, for certain particle-size/wavelength combinations, the radiation absorption and particle heating can be very non-uniform as a result of reflection, refraction, absorption, and interference of the radiation in the particle. They presented two parameters for use in determining when nonuniform heating is important

$$N = k_p \Delta T \lambda / 4 \pi a^2 n_m n_p \kappa_p I_0 \quad (2)$$

$$\tau_d = a^2 / \alpha_p \quad (3)$$

where N is the ratio of conduction to radiation deposition in the particle, and τ_d is a characteristic time scale for thermal diffusion in the particle. Here I_0 is the incident radiative flux (W/m^2), k the thermal conductivity, ΔT a characteristic temperature difference (e.g., the difference between the particle melting temperature and the ambient temperature), α the thermal diffusivity, and the other variables are as previously defined. The subscripts p and m refer to the particle and medium, respectively. When $N \geq 100$ and $\tau_p \geq \tau_d$, Tuntomo and Tien concluded that the lumped particle approximation is acceptable. Larger particles, shorter wavelengths, and shorter pulse widths prevent such an assumption; however, there is still a large range of particle-size/wavelength/radiant flux combinations of practical interest that do obey the above criteria; hence, we assume the particle absorption to be uniform with the caveat that the above conditions on N and τ_p are observed.

Another result of electromagnetic theory is that the effective absorption cross section of the particle can be significantly different from its geometric cross section.¹⁶ This occurs because of diffraction and interference effects as the radiation interacts with the particle. One can define an absorption cross section efficiency Q_a as

$$Q_a = C_a / \pi a^2 \quad (4)$$

where C_a is the effective absorption cross section of the particle. In Fig. 1, Q_a is plotted as a function of particle size for Pt in a glass medium for the wavelengths appearing in Table 1, taking into account Pt's wavelength-dependent optical properties. The calculations are from standard Mie scattering theory,¹⁶ and several points are worth noting. First, the effective cross section for small particles and long wavelengths can be 1/100,000 of the geometric cross section, resulting in a drastically smaller total energy absorption than if the geometric cross section is used. Also, for the case $a \ll \lambda$, Q_a becomes linear in a , and for $a \gg \lambda$, Q_a becomes constant. In general, however, there is no simple trend in the plots. Finally, Q_a depends strongly on the wavelength, which is due in part to the wavelength-dependent optical properties of Pt.

Model Formulation

Consider a homogeneous, spherical particle of radius a embedded in an infinite medium initially at a uniform tem-

Table 1 Optical properties of Pt for several wavelengths of interest

$\lambda, \mu\text{m}$	n	κ
0.5	2.0	3.4
1.0	3.5	5.7
5.0	4.7	19.4
10.0	10.0	36.0

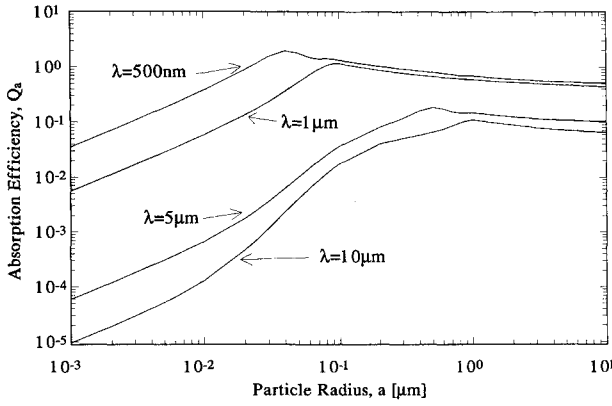


Fig. 1 Cross-sectional absorption efficiency Q_a as a function of particle radius a .

perature T_∞ . The particle is centered at the origin of a spherical coordinate system whose radial component is designated as r . At time $t = 0$, a constant-intensity, uniform radiation pulse of duration τ_p impinges upon the surface of the particle. The conservation of energy equations for the system are

$$\rho_m C_m \frac{\partial T_m}{\partial t} = k_m \frac{1}{r^2} \frac{\partial}{\partial r} \left(r^2 \frac{\partial T_m}{\partial r} \right) \quad (5)$$

$$\rho_p C_p V \frac{\partial T_p}{\partial t} = V q''' - A q'' \quad (6)$$

with initial and boundary conditions

$$T_p(t = 0) = T_\infty \quad (7)$$

$$T_m(r, t = 0) = T_\infty \quad (8)$$

$$T_m(r \rightarrow \infty, t) = T_\infty \quad (9)$$

$$T_p - T_m|_{r=a} = R_{bd} q'' = -R_{bd} k_m \frac{\partial T_m}{\partial r} \Big|_{r=a} \quad (10)$$

where T is the temperature, ρ the density, C the specific heat, and V and A are the volume and surface area of the particle, respectively. Also, q''' is the volumetric heat generation based on uniform radiation absorption, and $q'' = -k_m \partial T_m / \partial r|_{r=a}$ is the heat flux across the interface.

The energy equation for the particle is lumped in space because uniform radiation absorption within the particle has been assumed, as discussed in the previous section. This assumption is further justified as the thermal diffusivity of the particle is typically two orders of magnitude greater than that of the medium. As a result, the thermal energy diffuses throughout the particle much more quickly than it diffuses through the medium, which tends to redistribute moderate local temperature peaks in the particle before the bulk of the thermal energy begins its propagation into the medium.

The boundary resistance enters as the nonzero difference between the particle and medium temperatures at $r = a$ in Eq. (10). As explained above, this temperature difference is proportional to the heat flux across the particle-medium interface, which is equivalently expressed in terms of the medium temperature gradient evaluated at the particle surface, $r = a$.

The volumetric heat generation q''' accounts for the uniform absorption of incident radiation by the spherical particle. In practice, q''' is related to the incident radiative flux and the absorption cross-sectional efficiency as follows:

$$q''' V = \pi a^2 Q_a I_0 = \pi a^2 Q_a E_T / \tau_p \quad (11)$$

where E_T is the laser fluence (J/cm^2). The following nondimensional variables and parameters are introduced:

$$\theta = (T - T_\infty) / T_\infty, \quad t^* = t / \tau_p, \quad r^* = r / a \quad (12)$$

$$\gamma^2 = a^2 \rho_m C_m / \tau_p k_m, \quad \beta = 3 \tau_p k_m / \rho_p C_p a^2 \quad (13)$$

$$q = q''' \tau_p / T_\infty \rho_p C_p, \quad R = R_{bd} k_m / a \quad (14)$$

where r^* and t^* represent nondimensional distance and time, respectively.

The Laplace transform is used to remove the time dependence from the equations, and results in ordinary differential equations. The Laplace-transformed equations for the medium and particle, respectively, are [here, the bar ($\bar{}$) denotes the Laplace-transformed variable]

$$\frac{1}{r^{*2}} \frac{d}{dr^*} \left(r^{*2} \frac{d\bar{\theta}_m}{dr^*} \right) - \gamma^2 s \bar{\theta}_m = 0 \quad (15)$$

$$s \bar{\theta}_p - \frac{q}{s} - \beta \frac{d\bar{\theta}_m}{dr^*} \Big|_{r^*=1} = 0 \quad (16)$$

with boundary conditions

$$\bar{\theta}_m(r^* \rightarrow \infty, s) \rightarrow 0 \quad (17)$$

$$\bar{\theta}_p(s) - \bar{\theta}_m(r^* = 1, s) = -R \frac{d\bar{\theta}_m(r^*, s)}{dr^*} \Big|_{r^*=1} \quad (18)$$

Equations (15) and (16) are now coupled through the temperature gradient at the particle surface as a result of the TBR constraint, Eq. (18).

The solution to Eq. (15), after inserting boundary conditions (17) and (18), becomes

$$\bar{\theta}_m(r, s) = \frac{q e^{\gamma(1-r)\sqrt{s}}}{\gamma R r s} \left[\frac{\beta}{\gamma R} + \frac{\beta}{R} s^{1/2} + \frac{1+R}{\gamma R} s + s^{3/2} \right]^{-1} \quad (19)$$

The parenthesized portion of the denominator is a polynomial in $s^{1/2}$ and can be factored into the form $(s^{1/2} + d)(s^{1/2} + f)(s^{1/2} + g)$, where d , f , and g are the negatives of the roots of this polynomial. Upon expanding the factored polynomial by partial fractions, the inverse Laplace transform can be found in standard tables.¹⁸ The result for the particle temperature is

$$\begin{aligned} \theta_p(t) = & \frac{q}{\gamma R} \left[\frac{1+R}{dfg} + A(\gamma R d - R - 1) \right. \\ & \times e^{d^2 t} \text{erfc}(dt^{1/2}) + B(\gamma R f - R - 1) e^{f^2 t} \text{erfc}(ft^{1/2}) \\ & \left. + C(\gamma R g - R - 1) e^{g^2 t} \text{erfc}(gt^{1/2}) \right] \quad (20) \end{aligned}$$

where

$$\begin{aligned} A &= \frac{1}{d(d-f)(d-g)}, \quad B = \frac{-1}{f(d-f)(f-g)} \\ C &= \frac{-1}{g(d-g)(g-f)} \end{aligned} \quad (21)$$

and $\text{erfc}(z)$ is the complimentary error function.

It is assumed that the laser pulse repetition rate is much greater than the pulse duration, and that the system relaxes to equilibrium before the next pulse arrives; thus the model

considers only single pulse heating. Also, the maximum temperature rise in the system is assumed to occur at the end of the laser pulse; the model doesn't account for the cooling-down period after the laser pulse. Accordingly, the maximum particle temperature is calculated at $t^* = 1$ (i.e., the temperature at the end of the laser pulse) for a prescribed volumetric heat absorption q , which is proportional to the incident radiative flux [Eq. (11)]. Alternatively, the damage threshold fluence can easily be obtained by solving Eqs. (20) and (11) for E_T .

Damage Threshold Scaling

While the exact solution developed in the previous section accurately describes the effect of TBR on the particle heating, it is difficult to extract the functional relationship between important parameters of the problem and their effects on particle heating (which determines the damage threshold). For this reason, a scaling analysis is developed to predict the damage threshold as a function of pulse width, particle size, magnitude of the TBR, and material properties.

The lumped energy balance on a particle of radius a embedded in a host medium is considered, resulting in Eq. (6). The laser pulse duration τ_p imposes a characteristic time scale on the heat transfer. The largest particle temperature occurs at the end of the laser pulse; hence, the temporal derivative scales as¹⁹

$$\frac{\partial T_p}{\partial t} \sim \frac{\Delta T_p}{\tau_p} \sim \frac{T_c}{\tau_p} \quad (22)$$

where the ambient temperature is taken to be 0, and T_c is some critical temperature associated with damage to the particle and/or medium. It could, e.g., be the melting temperature of the particle and/or host, or the temperature at which mechanical stress in the system becomes intolerable. During this time energy will also diffuse away from the particle. Referring to Eq. (5), the characteristic diffusion length in the medium becomes $l \sim \sqrt{\alpha_m \tau_p}$. Here, l is a measure of how far away from the particle the bulk of the energy diffuses in a time τ_p . Then, the heat flux scales as

$$q'' = -k_m \left. \frac{\partial T_m}{\partial r} \right|_{r=a} \sim \frac{\Delta T}{R_{th}} \sim \frac{T_c}{R_{th}} \quad (23)$$

where

$$R_{th} = R_{bd} + l/k_m = R_{bd} + \sqrt{\alpha_m \tau_p}/k_m \quad (24)$$

represents both TBR and diffusion resistance in passing from particle to medium. Inserting the above expressions into the particle energy balance, Eq. (6), the following results:

$$E_T \sim \frac{4a\rho_p C_p T_c}{3Q_a} + \frac{4k_m \tau_p T_c}{Q_a(k_m R_{bd} + \sqrt{\alpha_m \tau_p})} \quad (25)$$

The first term on the right represents the internal energy storage of the particle and accounts for the particle temperature increase solely as a function of the total energy absorbed. Note the lack of a dependence on the pulse width. This is as expected since the rate of energy deposition is unimportant. The particle size dependence is captured in the ratio a/Q_a . The explicit linear relationship on the particle size a is not surprising since the volume/area ratio of a spherical particle $\sim a$. Larger particles heat up less than their smaller counterparts for a fixed input energy. In general, however, little can be said about E_T as a function of a due to the complicated dependence of Q_a on a . The second term on the right represents energy lost by the particle to the surrounding medium by conduction. A time dependence does appear here because the thermal gradients in the medium—which deter-

mine the heat flux, and hence, the particle temperature—are dependent on the pulse width as shown above.

The damage threshold depends on the dominant term in Eq. (25). Dividing the second term on the right by the first yields

$$\frac{3\sqrt{\alpha_m \tau_p}^{3/2}}{a(\tau_p + R_{bd}\sqrt{k_m \rho_m C_m})} \equiv \Gamma \quad (26)$$

where the fact that $\rho_m C_m \approx \rho_p C_p$ for many particle/medium material combinations is used. When $\Gamma \gg 1$, the particle energy storage is unimportant, and diffusion-limited phenomena dictate how easily the particle conducts away its heat energy. The second term in Eq. (25) thus determines how much the particle temperature rises for a given energy input, which will be called the *diffusion limit*. Likewise, when $\Gamma \ll 1$, the particle has difficulty dumping its energy—the medium offers a tremendous resistance to heat flow through it—and the particle is effectively insulated. Hence, only the total energy absorbed by the particle is important, and the first term in Eq. (25) represents the threshold limit. This limit is deemed the *insulating limit*. Based on the above, the damage threshold for both limiting cases is

$$E_T \sim \begin{cases} 4a\rho_p C_p T_c/3Q_a & \Gamma \ll 1 \\ \frac{4\tau_p^{3/2} T_c \sqrt{k_m \rho_m C_m}}{Q_a(\tau_p + R_{bd}\sqrt{k_m \rho_m C_m \tau_p})} & \Gamma \gg 1 \end{cases} \quad (27)$$

which is a convenient expression for determining the functional dependence of parameters of interest. Several words of caution are in order, however. First, there is a *strong* dependence of Q_a on a , although this is not immediately apparent from the above expression. One must first consult Fig. 1 to determine Q_a before using Eq. (27) to approximate E_T . Likewise, no explicit wavelength dependence appears in Eq. (27); however, Q_a also depends on the optical properties of the particle, which, for metals like Pt, are strongly wavelength dependent. Also, important assumptions have been made that depend on a and τ_p (and other variables) regarding uniform absorption and temperature within the particle and should be observed when using Eq. (27).

For the case $R_{bd} = 0$ and $\Gamma \gg 1$, the damage threshold scales as

$$E_T \sim 4T_p \sqrt{k_m \rho_m C_m \tau_p} / Q_a \quad (28)$$

which has been presented in similar form by other researchers,³ although the effective absorption cross section Q_a is not accounted for. For this case, the damage threshold depends on the square root of the laser pulse duration. It is noteworthy that this limit is not valid for $\Gamma \ll 1$, which occurs for large particles, short laser pulses, and/or high thermal boundary resistance.

Another interesting limiting case is when

$$R_{bd}\sqrt{k_m \rho_m C_m}/\sqrt{\tau_p} \gg 1 \quad \text{and} \quad \Gamma \gg 1 \quad (29)$$

In this case

$$E_T \sim 4\tau_p/R_{bd} \quad (30)$$

Here, the damage threshold dependence on the laser pulse width becomes more acute—a linear relationship exists between the two. Note, however, that Γ is also affected by the $R_{bd}\sqrt{k_m \rho_m C_m}/\tau_p$ term; when this becomes large compared to one, Γ tends to become small, bringing the alternate limiting phenomena into play. These examples illustrate that the damage threshold can depend on the pulse width over a range of values: $E_T \sim \tau_p^r$, where $0 \leq r \leq 1$, depending on the parameters of the problem.

Results and Discussion

In this section, results from both the exact solution and scaling are presented over a range of practical interest. Regime maps from the scaling relations are constructed based on the particle size, laser pulse width, and magnitude of the TBR. A typical calculation for the particle temperature rise is performed with the exact solution. The particle temperature is considered here, however, the analysis also yields the medium temperature field, and the following results can equally be expressed in terms of the host temperature $T_m(r, t)$, with an associated damage threshold temperature for the host.

Three parameters of interest are considered here: 1) the laser pulse width τ_p ; 2) boundary resistance R_{bd} ; and 3) particle size a . Pulse widths from 10 ps (10^{-11} s) through 100 ns (10^{-7} s) are examined. For a fixed laser pulse energy, longer pulses result in temperature profiles that approach the conventional solution ($R_{bd} = 0$). This occurs because the heat flux decreases as the pulse width increases, and the temperature drop across the particle/medium interface is proportional to the heat flux across it. Shorter pulses are avoided because the laser-material interactions become much more complicated as the laser pulse width approaches the molecular time scales of the particle/host material.²⁰

Swartz and Pohl⁵ report measured values of R_{bd} for a $\text{Rh}_{99.5}\text{Fe}_{0.05}/\text{SiO}_2/\text{Al}_2\text{O}_3$ interface. As the data in their work indicates, Pt and Rh result in similar values of the TBR as computed from both the acoustic mismatch theory and diffuse mismatch theory. Thus, the measured values of R_{bd} on SiO_2 for Rh:Fe are used for the Pt particle embedded in SiO_2 . Extrapolating their values from 200 K to room temperature, R_{bd} is found to be on the order of 10^{-7} – 10^{-8} $\text{K}\cdot\text{m}^2/\text{W}$; hence, results are reported for values in this range. The data are for flat interfaces, yet the particle/medium interface is curved. If the mean free path of the energy carriers in the particle and medium (e.g., electrons, phonons, etc.) is much smaller than the particle radius, then the geometry of the interface is immaterial. Otherwise, the influence of the interface curvature remains to be investigated.

The range of particle sizes is taken to be 10^{-5} – 10^{-8} m. Campbell et al.¹³ reported that particles on the order of several microns in size have been observed in the optical components of their high-power laser system, which is used as the large particle size limit for calculations. The particle size limit of 10^{-8} m is chosen arbitrarily.

Figure 2 is a log-log plot of the Γ vs R_{bd} , for different τ_p and a particle size of $a = 10^{-7}$ m. As R_{bd} increases and τ_p decreases, Γ decreases and the damage threshold approaches the insulating limit. Increasing R_{bd} increases the resistance to heat transfer from particle to medium directly, and as τ_p decreases the thermal gradient in the medium increases, posing additional resistance to heat transfer. Figure 3 is a similar plot of Γ vs τ_p for different particle sizes and $R_{bd} = 10^{-7}$ $\text{K}\cdot\text{m}^2/\text{W}$. Here, both increasing a and decreasing τ_p yields a decrease

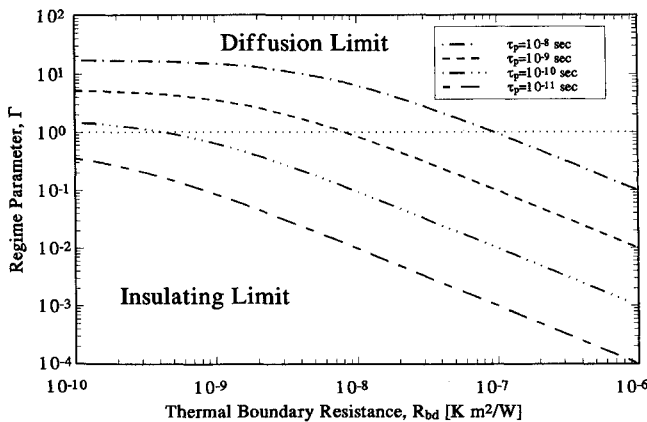


Fig. 2 Γ vs R_{bd} .

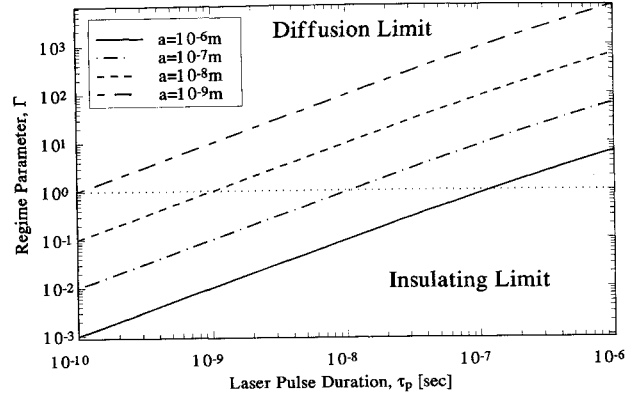


Fig. 3 Γ vs τ_p .

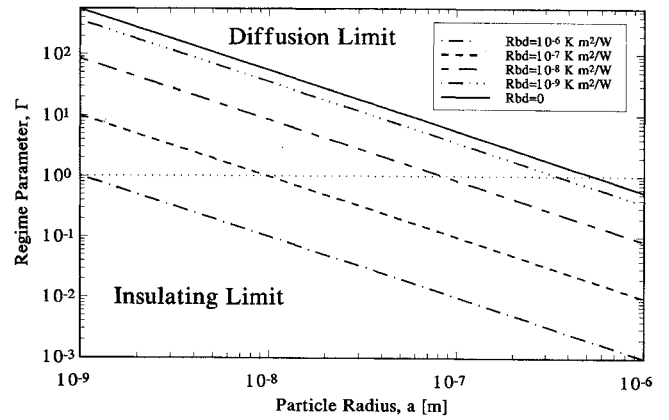


Fig. 4 Γ vs a .

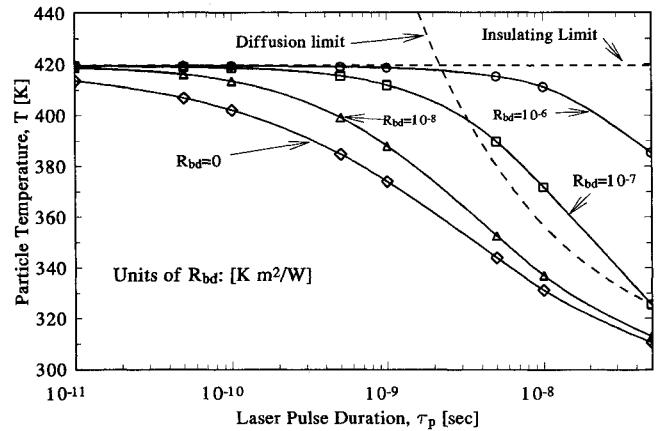


Fig. 5 Temperature rise as a function of laser pulse width τ_p .

in Γ , and again, the insulating limit prevails. The variation in Γ with a is related to the volume/area ratio a as discussed earlier: larger particles have a higher E_T for the insulating case, which decreases Γ . Observe that the absorption cross section efficiency does not effect the dominant heating mechanism parameter in Eq. (26). This happens because Γ determines what happens *after* the energy has entered the particle and is not concerned with how it initially gets there. Figure 4 plots the variation in Γ with a for several values of R_{bd} and a pulse width of 10^{-9} s.

Figure 5 shows the particle temperature variation vs the laser pulse duration τ_p as calculated from the analytic solution, Eq. (20), for a typical situation. The parameters used in this calculation appear in Table 2.

Plots for $R_{bd} = 0, 10^{-8}, 10^{-7}$, and 10^{-6} $\text{K}\cdot\text{m}^2/\text{W}$ are shown along with both the diffusion limit and the insulating limit. In each case, a fixed energy of 1 pJ (1×10^{-12} J) is uniformly

Table 2 Parameters used in particle temperature calculation

Parameter	Value	Units
$\rho_p C_p$	2×10^6	$\text{J/m}^3 \times \text{K}$
$\rho_m C_m$	2×10^6	$\text{J/m}^3 \times \text{K}$
k_p	100	$\text{W/m} \times \text{K}$
k_m	1	$\text{W/m} \times \text{K}$
T_∞	300	K
a	10^{-7}	m

absorbed by the particle over the duration of the laser pulse. The plots represent the temperature of the particle at the end of the laser pulse accounting for diffusion into the medium and a nonzero thermal boundary resistance. As the pulse width decreases, the heat flux to the particle increases accordingly. The constant line at $T_p \approx 420$ K is the insulating limit and represents the maximum attainable temperature of the particle. In this case, no energy at all leaves the particle, and the entire laser pulse contributes to its temperature rise. Also plotted is the diffusion limit from the prior scaling: $T_p \sim E_T/\sqrt{\tau_p}$ with $R_{bd} = 0$. The actual temperature follows the heating limit in Eq. (27) (i.e., diffusion limit vs insulation limit) that yields the lowest temperature rise for a given pulse energy. Furthermore, the temperature varies linearly with the total energy absorbed; thus, changing the total energy input will change the absolute temperature distributions, but the temperature to heat input ratio $T_p/q''V$ remains the same.

Several interesting points are worth noting. First, T_p approaches the maximum possible temperature as $\tau_p \rightarrow 0$, which represents the insulating limit and agrees with the scaling results. Likewise, for small values of R_{bd} , as τ_p increases, T_p approaches the diffusion limit, also as expected. Note that larger values of R_{bd} result in higher particle temperatures for a given pulse width and energy, which also is as expected. Furthermore, as R_{bd} becomes small, the temperature profile approaches that for $R_{bd} = 0$. Finally observe that, even for moderate values of R_{bd} , the temperature change considering the thermal boundary resistance can exceed that predicted from the conventional theory by a factor of two or more. As R_{bd} increases this difference becomes even more pronounced.

Conclusions

The preceding work develops an inclusion-based laser damage model that incorporates the TBR experienced at the particle/medium interface. Sources of the TBR are discussed. The heat transfer from a spherical absorbing particle embedded in a nonabsorbing host medium is mathematically modeled using Fourier conduction. Mie theory is used to calculate the effective cross section, and the requirements for uniform absorption in the particle are stated.

An exact solution to the governing equations is obtained by solving the conservation of energy equations for both the particle and medium. The Laplace transform is used to obtain the exact solution for the temperature rise of the particle as a function of the incident radiation fluence and pulse width. In all cases, the TBR increases the temperature rise of the particle. The results indicate that the predicted particle temperature rise can be over twice as large as that when the TBR is neglected.

A basic scaling analysis is also performed to determine the nature of the heating process. This analysis is based on laser pulse width, magnitude of the TBR, particle size, and material properties. These scaling results reveal two distinct limits on the damage threshold: the insulating limit and the diffusion limit. A single parameter is defined that determines which limit governs the heat transfer process. Graphs of this param-

eter are plotted as a function of TBR, laser pulse width, and particle size. The scaling laws predict the same trends found in the exact solution. It is shown that the presence of the TBR can increase the damage threshold dependence on pulse width beyond the square root relationship encountered in the literature.

Acknowledgments

The authors acknowledge the financial support from the U.S. National Science Foundation and the U.S. Department of Energy.

References

- ¹Akhmanov, S. A., Vysloukh, V. A., and Chirkin, A. S., *Optics of Femtosecond Laser Pulses*, American Inst. of Physics, New York, 1992, p. 335.
- ²Walker, T. W., Guenther, A. H., and Nielsen, P., "Pulsed Laser-Induced Damage to Thin-Film Optical Coatings—Part II: Theory," *IEEE Journal of Quantum Electronics*, Vol. 17, No. 10, 1981, pp. 2053–2065.
- ³Guenther, A. H., and McIver, J. K., "The Pulsed Laser Damage Sensitivity of Optical Thin Films, Thermal Conductivity," *Laser and Particle Beams*, Vol. 7, No. 3, 1989, pp. 433–441.
- ⁴Koldunov, M. F., Manenkov, A. A., and Pokotilo, I. L., "The Theory of Inclusion-Initiated Laser Damage in Optical Materials: The Thermal Explosion Mechanism," *Laser Induced Damage in Optical Materials: 1988*, 1988 NIST Spec. Pub. 775, Washington, DC, 1989, pp. 502–515.
- ⁵Swartz, E. T., and Pohl, R. O., "Thermal Resistance at Interfaces," *Applied Physics Letters*, Vol. 51, No. 26, 1987, pp. 2200–2202.
- ⁶Fletcher, L. S., "Recent Developments in Contact Conductance Heat Transfer," *Journal of Heat Transfer*, Vol. 110, No. 4B, 1988, pp. 1059–1070.
- ⁷Tio, K., and Sadhal, S. S., "Thermal Constriction Resistance: Effects of Boundary Conditions and Contact Geometries," *International Journal of Heat and Mass Transfer*, Vol. 35, No. 6, 1992, pp. 1533–1544.
- ⁸Kittel, C., *Introduction to Solid State Physics*, 6th ed., Wiley, New York, 1986, Chaps. 4 and 5.
- ⁹Swartz, E. T., and Pohl, R. O., "Thermal Boundary Resistance," *Reviews of Modern Physics*, Vol. 61, No. 3, 1989, pp. 605–668.
- ¹⁰Pettersson, S., and Mahan, G. D., "Theory of the Thermal Boundary Resistance Between Dissimilar Lattices," *Physical Review B*, Vol. 42, No. 12, 1990, pp. 7386–7390.
- ¹¹Majumdar, A., "Effect of Interfacial Roughness on Phonon Radiative Heat Conduction," *Journal of Heat Transfer*, Vol. 113, No. 4, 1991, pp. 797–805.
- ¹²Hopper, R. W., and Uhlmann, D. R., "Mechanism of Inclusion Damage in Laser Glass," *Journal of Applied Physics*, Vol. 41, No. 10, 1970, pp. 4023–4037.
- ¹³Campbell, J. H., Rainer, F., Kozlowski, M., Wolfe, C. R., Thomas, I., and Milanovich, F., "Damage Resistant Optics for a Mega-Joule Solid-State Laser," *Laser Induced Damage in Optical Materials: 1990*, 1990 SPIE Spec. Pub. 1441, Washington, DC, 1990, pp. 444–456.
- ¹⁴Weast, R. C., *CRC Handbook of Chemistry and Physics*, 67th ed., CRC Press, Boca Raton, FL, 1986, Sec. E.
- ¹⁵Fuka, M. Z., McIver, J. K., and Guenther, A. H., "Effects of Thermal Conductivity and Index of Refraction Variation on the Inclusion Dominated Model of Laser-Induced Damage," *Laser Induced Damage in Optical Materials: 1989*, 1989 NIST Spec. Pub. 801, Washington, DC, 1989, pp. 576–583.
- ¹⁶Bohren, C. F., and Huffman, D. R., *Absorption and Scattering of Light by Small Particles*, Wiley, New York, 1983, Chaps. 2–5.
- ¹⁷Tuntomo, A., and Tien, C. L., "Transient Heat Transfer in a Conducting Particle with Internal Radiant Absorption," *Journal of Heat Transfer*, Vol. 114, No. 2, 1992, pp. 304–309.
- ¹⁸Beyer, W. H., *CRC Standard Mathematical Tables*, 27th ed., CRC Press, Boca Raton, FL, 1984, p. 419.
- ¹⁹Bejan, A., *Convective Heat Transfer*, Wiley, New York, 1984, pp. 17–21.
- ²⁰Oiu, T., and Tien, C. L., "Short-Pulse Laser Heating on Metals," *International Journal of Heat and Mass Transfer*, Vol. 35, No. 3, 1992, pp. 719–726.